第17回性能に基づく橋梁等の耐震設計に関する
シンポジウム講演論文集（2014年7月）

Analytical Evaluation on Influence by M-N Interaction on Failure Mechanisms of A Rigid-Frame Arch Bridge

Zhongqi SHI[1], Kenji KOSA[2], Jiandong ZHANG[3] and Tatsuo SASAKI[4]

[1]Student Member of JSCE, Ph. D. Candidate, Grad. School of Eng., Kyushu Institute of Technology
(Sensui-cho 1-1, Tobata-ku, Kitakyushu, Fukuoka, 804-0015, Japan)
[2]Member of JSCE, Ph. D., Prof. Dept. of Civil Eng., Kyushu Institute of Technology
(Sensui-cho 1-1, Tobata-ku, Kitakyushu, Fukuoka, 804-0015, Japan)
[3]Member of JSCE, Senior Engineer, Jiangsu Transportation Research Institute
(2200, Chengxin Road, Jiangning Science Park, Nanjing, 211112, China)
[4]Member of JSCE, Manager, Technical Generalization Division, Nippon Engineering Consultants Co., Ltd.
(Currently in the doctoral program at Kyushu Institute of Technology)

1. INTRODUCTION

Wenchuan Earthquake occurred in Sichuan Province, China, at 2:28 p.m. on May 12th, 2008. It had the magnitude of 8.0 measured by CEA (China Earthquake Administration) and 7.9 by USGS (US Geographical Survey). Great damage occurred to highway bridges. Arch bridge is a widely favorable bridge type in China for a long time, and has been abundantly constructed. During the Wenchuan Earthquake, arch bridges also suffered noticeable damage.

Authors conducted field damage surveys of Xiaoyudong Bridge (shown in **Fig. 1**), which is a RC rigid-frame arch bridge. By study[1)] on this bridge type, it is a composite structural type of arch bridge and inclined rigid-frame bridge, and a static indeterminate structure, constructed in China since 1980s abundantly. By statistical investigation, accumulative total span length of this type of bridge is more than 15,000 km. Xiaoyudong Bridge is the only RC rigid-frame arch bridge that collapsed in Wenchaun Earthquake. However, there is still few detailed research on its vibration behavior.

Besides, it is widely understood that the moment-axial load (M-N) interaction, also known as the effect by fluctuation of axial load, plays a very important role in the vibration phenomenon of RC arch bridges. On the topic of the influence to the seismic behavior of RC arch bridge by considering or neglecting the M-N interaction,

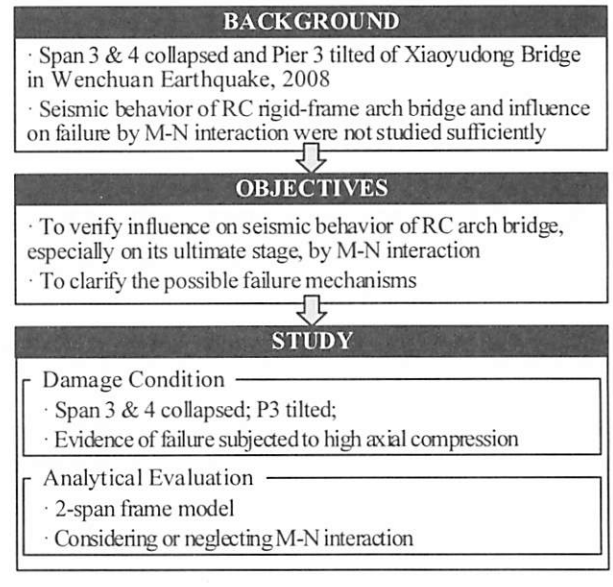

Fig. 2 Study Flow

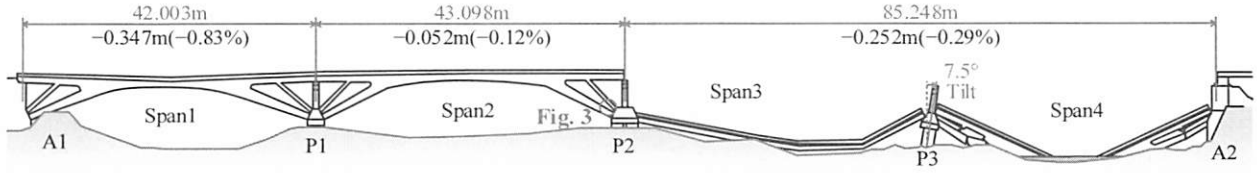

Fig. 1 Elevation View of Xiaoyudong Bridge after the Earthquake (view from upstream)

several studies have been conducted. Evaluations by frame model (M-Φ relationship) considering/neglecting axial load fluctuation are published (example as Ref (2)). However, only the influence on responses for yield stage are discussed. On the other hand, assessments (example as Ref (3)) are also performed by comparing case with M-N interaction (by fiber model with σ-ε relationship) with case neglecting M-N interaction (by frame model with M-Φ relationship). However, not only the consideration of M-N interaction, but the differences of σ-ε relationship, M-Φ relationship and hysteresis may also affect the analytical results, which are failed to be clarified in these studies. It should be noticed as well that in all these references[2~3], the fluctuation of axial load is not extremely extensive, and does not exceed 30% of axial capacity in the M-N diagram. However, arch leg of Xiaoyudong Bridge stands 30.3% axial compression under only dead load. By pre-analysis, axial load may vary by about ±35%. Thus, it is necessary to study the effect of M-N interaction on this brittle structure.

Study flow is shown in **Fig. 2**. Aiming at verifying its inplane vibrate behavior, and clarifying the possible failure mechanisms, nonlinear dynamic analyses by 2-span frame model are conducted. Then, the influence by considering or neglecting the M-N interaction, with attention paid on the ultimate stage and the local failure, is also evaluated in this paper.

2. OBJECTIVE BRIDGE

The structure of Xiaoyudong Bridge and its damage condition have been described in former paper[4] in details. All abutments, piers and spans are numbered from the left bank, as shown in **Fig. 1**. Furthermore, key members are numbered as well, in terms of "position" - "span No." - "left/right". For instance, AL-3-L, IL-3-L and G-3-L respectively stands for bottom of arch leg, bottom of inclined leg and girder joint, on left of Span 3.

It should be specially noticed that, being the main supporting member, arch leg has relatively small section (350mm * 720mm) as shown in **Fig. 3**, and the tie ratio of this member is very low (0.16%). From **Fig. 3**, it can be found that one visible crack occurred at bottom of arch leg on the right side of Span 2 (AL-2-R), and spalling of concrete with 260mm (0.36 times of sectional depth) and 92mm (0.13 times of sectional depth) respectively occurred to upper and lower surface of AL-2-R. This phenomena, few cracks but notable spalling of concrete, suggests the arch leg might suffer great axial compression.

3. ANALYTICAL MODEL AND CONDITIONS

For studying the failure mechanisms of Span 3 & 4, as well as the possible influence by variation of axial load (considering or neglecting M-N interaction), 2-span

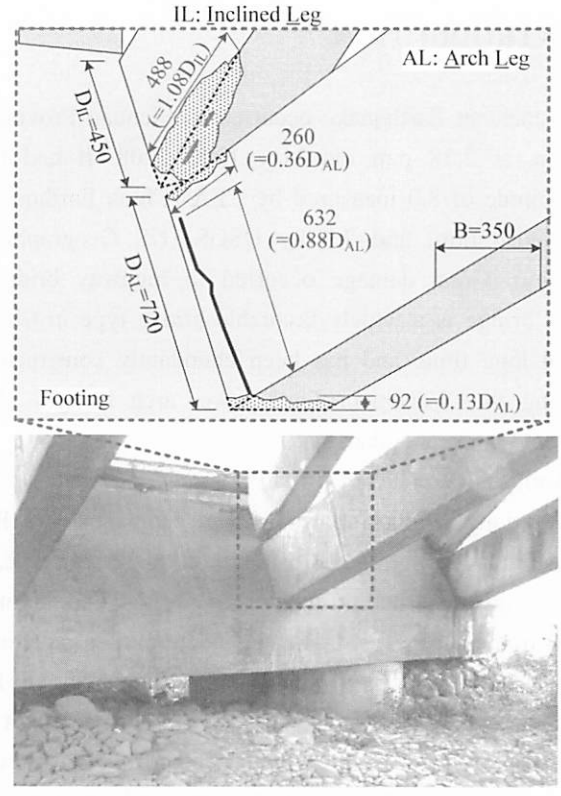

Fig. 3 Actual Damage at Bottom of Legs (AL-2-R and IL-2-R)

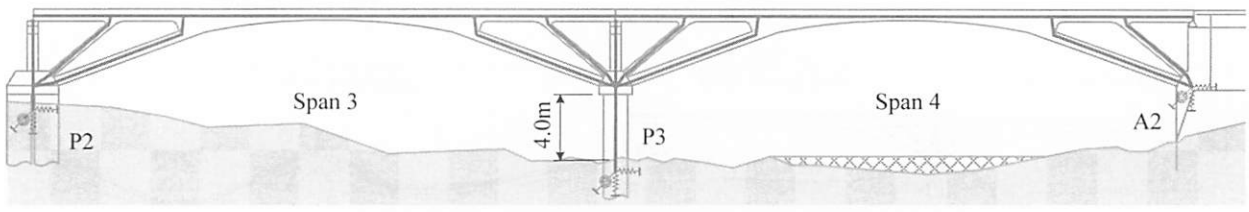

Fig. 4 Analytical Model for Span 3 & 4

frame model is established. As shown in **Fig. 4**, among five arch frames on transversal direction, one single arch frame is selected, including slab, to establish 2D model. Rigid elements have been set to the following parts: the footing, the beam on the top of the piers and the joints between legs and girder. Tri-linear M-Φ elements calculated based on Japanese specification are used for girder and inclined legs, considering axial forces when only dead load acts on the structure.

Furthermore, special attention is paid on arch legs, whose response axial load was found significant in preanalysis. Response range of flexural moment-axial load (M-N) at right bottom of arch leg on Span 4 (AL-4-R) is shown in **Fig. 5**. Here, axial resistance subjected to only compression is defined as maximum axial compressive load ($N_{max} = bd*f_c$). It can be got that, when only dead load acts on the bridge (noted as Point A) the axial load on arch leg is 1396 kN (30.3% N_{max}); axial load at peak of ultimate moment (M_{peak}, noted as Point B) is 1850 kN (40.1% N_{max}); and maximum response axial load (noted as Point C) is 2991 kN (64.8% N_{max}). This indicates that moment-axial load (M-N) interaction on arch leg may have inneglectable influence, and should be taken into account. Thus, bi-linear moment-curvature (M-Φ) relationship under variable axial load (N) is calculated. Here, Hoshikuma equation is applied for σ-ε relationship for concrete, thanks to its good applicability to low tie ratio members (ρ_t is only 0.16% for arch leg). Then, the calculated M_y-N and M_u-N are illustrated in **Fig. 5**. Correspondingly, the M-Φ relationship under three axial load conditions and N-Φ interaction curves are shown in **Fig. 6** (a) and (b) respectively. It can be observed that, from Point A to Point B, resistance moment increases slightly due to greater axial load, while the ultimate curvature (Φ_u) drops from 0.00860 1/m to 0.00688 1/cm; as axial load increases after the peak point until Point C, moment resistance begins to decrease, while the ultimate curvature (Φ_u) drops further from 0.00688 1/m to 0.00467 1/cm. This ultimate curvature (Φ_u) under maximum response axial load is only about half of that under only dead load. In this paper, case study is conducted by the comparison between the analysis based on M-Φ relationship under only dead load (A in **Fig. 5** and **Fig. 6**), and the analysis based on M-Φ relationship considering variation of axial load.

For the boundary conditions, vertical, horizontal and rotational springs are set under piers and abutments. For springs between girder and pier, a frictional spring which

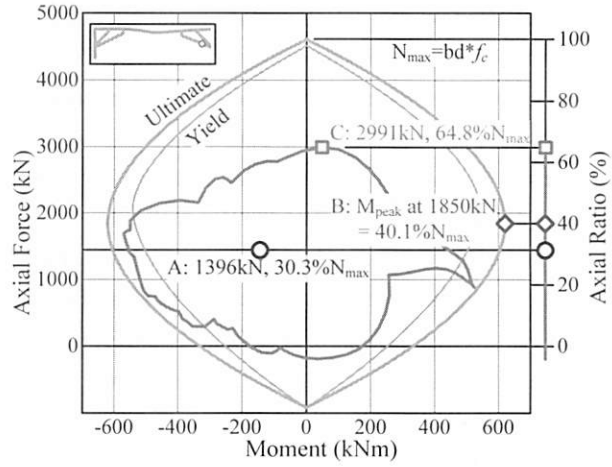

Fig. 5 M-N response range (AL-4-R)

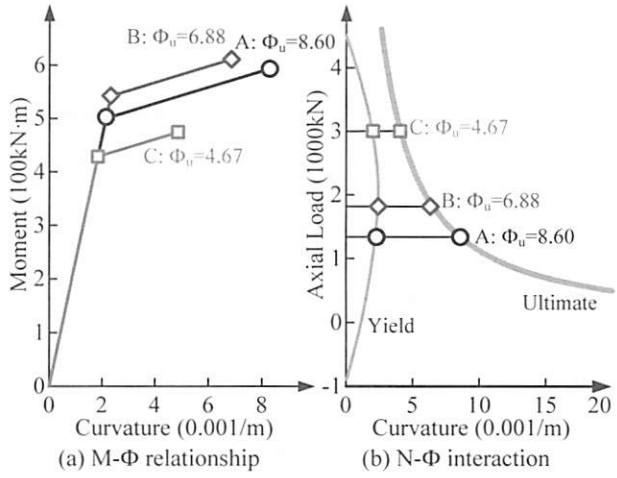

Fig. 6 Input M-N-Φ Interaction

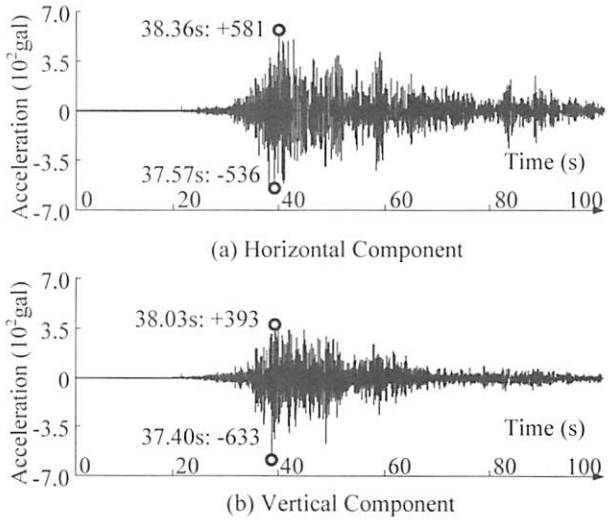

Fig. 7 Input seismic wave form (Bajiao)

is assumed to be comparatively weak, and a supporting spring are used on pier. On the other hand, frictional and supporting springs are used on top of abutment. Currently, collision spring is not taken into account. The exposure of P3 before the earthquake is also considered.

Thanks to the closest distance from Xiaoyudong Bridge (24 km), seismic wave by Bajiao Station is used in analyses. Recorded accelerations are shown in **Fig. 7**. Its peak acceleration of +581gal occurred at 38.36s, and -633gal occurred at 37.40s, for E-W and U-D respectively. Damping coefficient of 20% and 2% is separately utilized for springs at basement and all other concrete elements. Rayleigh damping based on eigen-vibration analysis is applied. The 1st and 10th modes are used for Rayleigh damping, for their great mass ratio. The analysis starts from 0.0s and ends at 100.0s. For the calculation, Newmark-β (β = 1/4) method is applied in the numerical integration, with the time step being 1/1000s.

4. ANALYTICAL RESULTS

By using the analytical model introduced above, dynamic analyses are conducted for cases considering or neglecting the M-N interaction. In this chapter, analytical results will be explained for member level in Section (1) in detail, followed by the general result in Section (2).

(1) Influence on Legs by M-N Interaction on Arch Leg

The response moment-curvature-axial load history (M-Φ-N) at bottom of right arch leg of Span 4 (AL-4-R) is summarized in **Fig. 8**. In this figure, curvature history and moment history is shown in (a) and (b) respectively, followed by M-Φ history in (c), and the interaction of M-N and N-Φ histories are shown in (d) and (e), with the comparison between the cases in which the M-N interaction of arch leg is considered or neglected. Here, some important events are defined (supertitle of comma

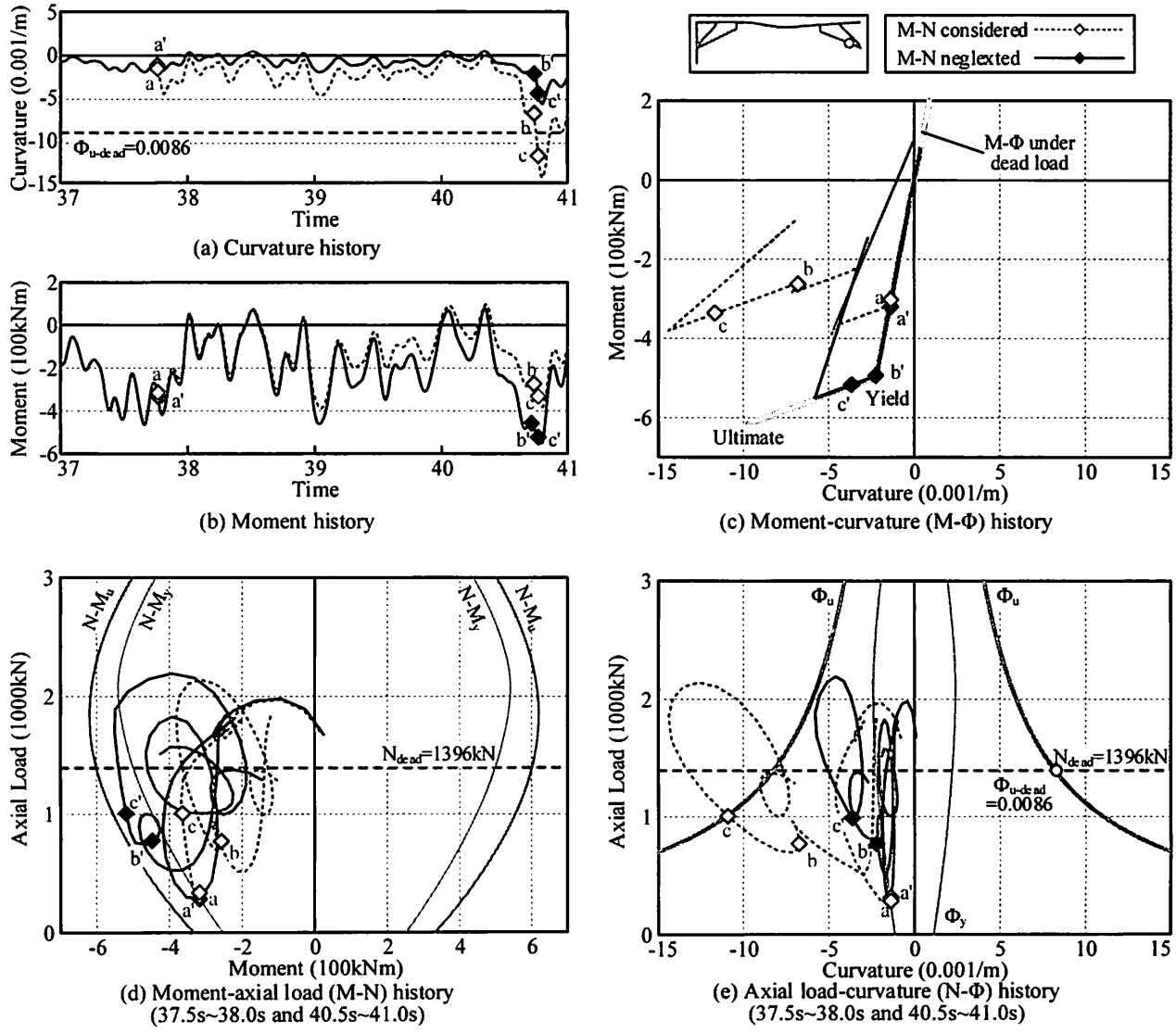

Fig. 8 Influence on Flexural Response due to M-N Interaction (AL-4-R)

stands for the result by neglecting the M-N interaction): a and a' for the time point when AL-4-R reaches yield in the case that considers the M-N interaction; b and b' for the time point when AL-4-R reaches yield in the case that neglects the M-N interaction; and c and c' for the time point when AL-4-R reaches yield in the case that considers the M-N interaction. The history during the time span from 37.0 sec to 41.0 sec is shown.

It can be found in **Fig. 8** (a) and (e) that by axial load due to only dead load (N_{dead}=1396 kN), the ultimate curvature of arch leg ($\Phi_{u\text{-}dead}$) is 0.0086 1/m. At Point a (37.77 sec), the response curvature by considering the M-N interaction reaches the yield curvature due to smaller flexural resistance under smaller axial load (297 kN, about 21% of N_{dead}) at that time point. Therefore, the response curvature from a to b is generally greater than that from a' to b' (in **Fig. 8** (a), (c) and (e)) because the earlier yield results in more obvious residual flexural deformation by considering M-N interaction, while the response moment from a to b is generally smaller than that from a' to b' (in **Fig. 8** (b), (c) and (d)). Then, AL-4-R reaches yield at Point b' (40.74 sec) by neglecting M-N interaction. At this time point, the response curvature by considering the M-N interaction (0.0079 1/m) is already as 3.6 times great as the response curvature by neglecting the M-N interaction (0.0022 1/m). After that, flexural response increases in both cases and ultimate stage is reached at Point c (40.77 sec) under axial load of 1048 kN (about 75% of N_{dead}). Also from **Fig. 8** (e), it can be observed that the flexural response of AL-4-R by considering the M-N interaction exceeds the Φ_u-N curve significantly, probably due to the earlier yield under low axial load. On the other hand, the response curvature of AL-4-R by neglecting the M-N interaction does not exceed the ultimate curvature of arch leg ($\Phi_{u\text{-}dead}$) of 0.0086 1/m until the end of analysis.

Furthermore, the response of bottom of left arch leg of Span 4 (AL-4-L) is summarized in **Fig. 9** as well. The history during the time span from 40.0 sec to 43.0 sec is shown as representative. From **Fig. 9** (a), we can see that the response curvature history is almost same by considering or neglecting the M-N interaction, since the yield has been reached under similar axial load condition in both cases. However, due to the fluctuation of axial load in arch leg, the ultimate curvature fluctuates notably (shown as the gray dotted line). In **Fig. 9** (b), the ultimate ratio is defined as the result that the response curvature divided by the ultimate curvature varied with the

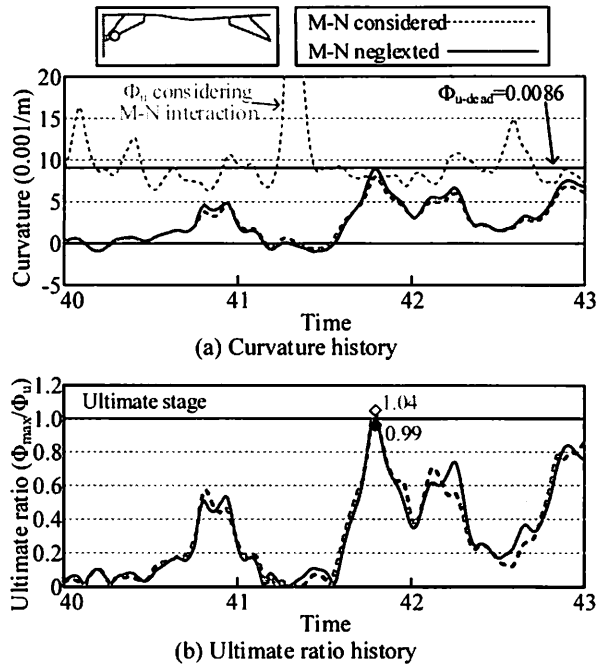

Fig. 9 Influence by M-N interaction (AL-4-L)

response axial load at any time point for the case in which the M-N interaction is considered, and the result that the response curvature divided by the ultimate curvature ($\Phi_{u\text{-}dead}$) the axial load due to only dead load for the case in which the M-N interaction is neglected. At 40.78 sec (in **Fig. 9** (a)), the response curvature by considering the M-N interaction exceeds the ultimate curvature (0.0077 1/m, about 90% of $\Phi_{u\text{-}dead}$) under axial load of 1639 kN (about 117% of Ndead). About 1.04 times of the ultimate curvature (defined as the ultimate ratio) is reached, as shown in **Fig. 9** (b). It suggests that AL-4-L reaches the ultimate stage by considering the M-N interaction because the ultimate curvature decreases under axial load which is greater than that under only dead load. On the contrary, by neglecting the M-N interaction, maximum ultimate ratio of 0.994 is got, and the ultimate curvature of arch leg ($\Phi_{u\text{-}dead}$) of 0.0086 1/m has not been reached until the end of analysis.

(2) Influence on General Results

To sum it up, the ultimate ratio at bottom of all arch legs (AL-3-L and AL-3-R for Span 3, AL-4-L and AL-4-R for Span 4) are calculated similarly to that in **Fig. 9** (b). The maximum ultimate ratio at 4 points are plotted in **Fig. 10**, with the comparison between that by considering or neglecting the M-N interaction for arch legs. It can be found that for the case in which the M-N interaction is considered, all 4 points have the ultimate ratio greater than 1.0, suggesting that the ultimate stage is reached at

all 4 points. The greatest value is 2.991 at AL-4-R, where the yield occurred very early due to decrease of yield resistance by decrease of response axial load. Besides, the average ultimate ratio of 4 points is 1.710 by considering M-N interaction (in **Fig. 10**). On the other hand, for the case in which the M-N interaction is neglected, only 1 of 4 points (AL-3-L) exceeds ultimate stage slightly, with the ultimate ratio being 1.063. All ultimate ratios of other 3 points (respectively 0.978, 0.994 and 0.767) are smaller than 1.0, not reaching ultimate stage. Furthermore, the average ultimate ratio is 0.950 by neglecting M-N interaction, which is smaller by 44% than that by considering M-N interaction (1.710). It can be concluded that no matter whether the yield occurs to section under axial load greater or smaller than the axial load by only dead load, the maximum flexural response would be underestimated if neglecting the M-N interaction, mainly because of the obvious decrease of ultimate curvature caused by increase of axial load.

Then, general ultimate ratio distribution is compared in **Fig. 11**. For girder shown in **Fig. 11** (a), it can be observed that the maximum ultimate ratio is similar. By considering the M-N interaction, the maximum ultimate ratio at Point G-4-L and G-4-R is 1.40 and 1.20 respectively (0.0394 1/m and 0.0338 1/m). On the other hand, by neglecting the M-N interaction, the value becomes 1.37 and 1.25 respectively (0.0386 1/m and

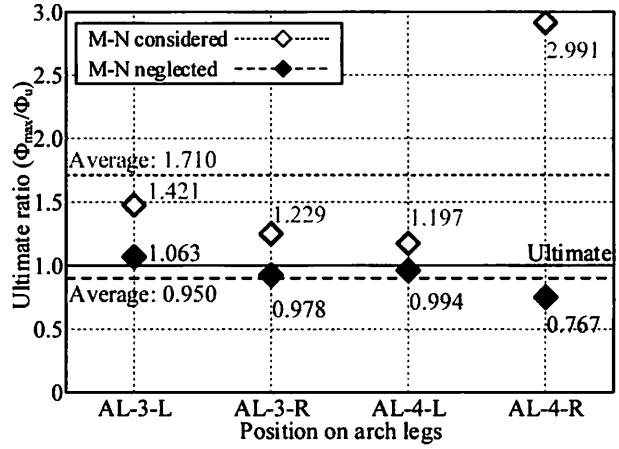

Fig. 10 Comparison of Ultimate Ratio of Arch Legs by Considering or Neglecting M-N Interaction

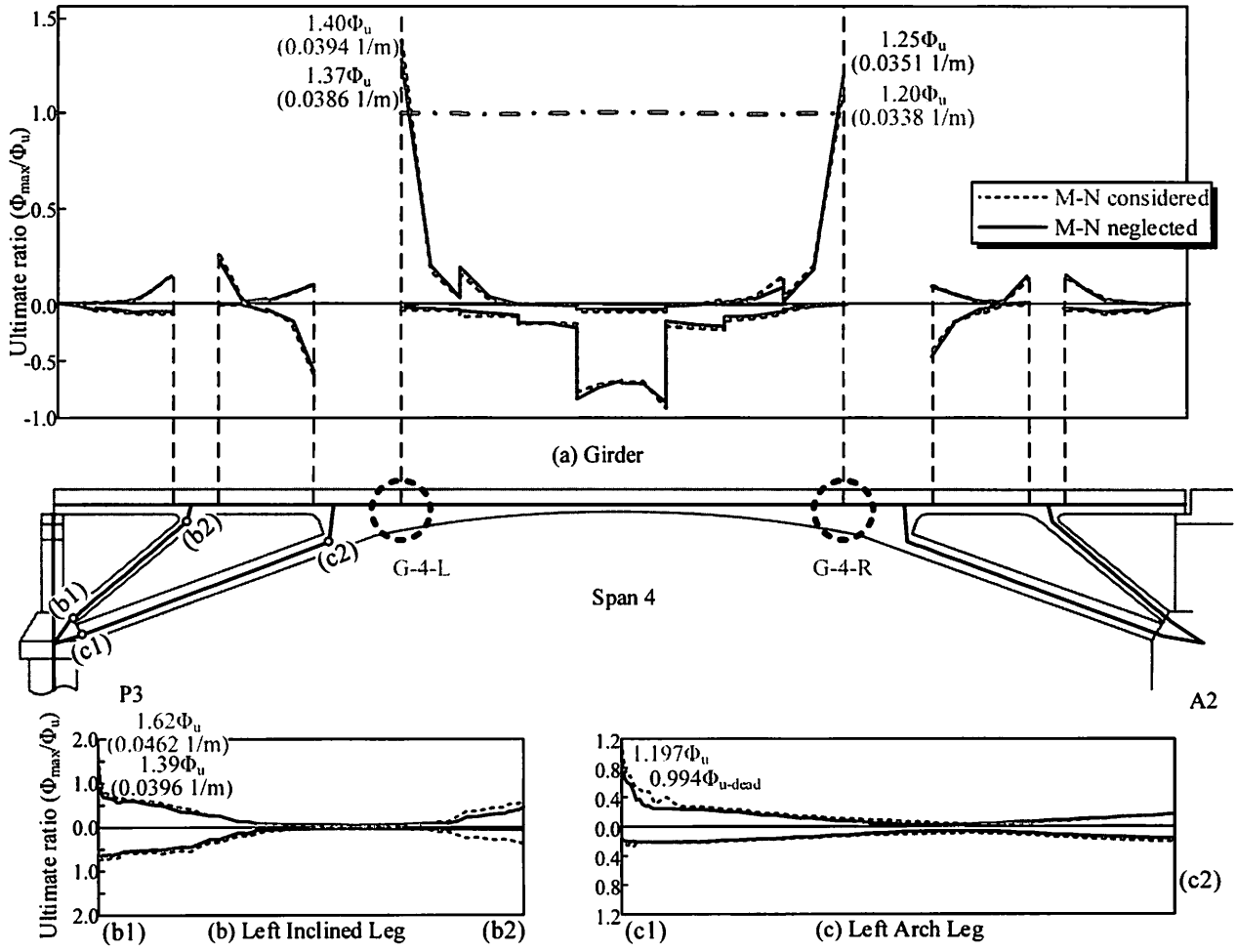

Fig. 11 Comparison of Ultimate ratio by Considering or Neglecting M-N Interaction

0.0351 1/m). Difference of ultimate ratio is relatively notable at bottom of legs. For bottom of left inclined leg, the maximum ultimate ratio is 1.62 (0.0462 1/m) by considering M-N interaction and 1.39 (0.0396 1/m) by neglecting that. For bottom of left arch leg, the value is 1.197 by considering M-N interaction and 0.994 by neglecting that. Therefore, by considering the M-N interaction, the maximum ultimate ratio is 16.5% and 20.4 % greater respectively at bottom of left inclined leg and left arch leg. It indicates that the influence on flexural response by considering or neglecting M-N interaction, will be notable for bottom of legs, but limited for girder.

5. FAILURE MECHANISMS

Based on the analytical result stated above, failure mechanisms is estimated in this chapter.

To explain the possible failure mechanisms, simplified 1/2-span mechanical model, with one set of inclined leg, arch leg, and a half of girder, is applied. Thus, the possible failure mechanisms are illustrated in **Fig. 12** for for Span 4 (represented by the right half span). Ultimate stage occurred at G-4-R, IL-4-R and AL-4-R, leading to violent vibration of the structure. As shown in **Fig. 12** (a), due to clockwise movement of legs, girder moved toward A2 for maximum 3.69 cm at 41.35s, and girder had possibility to collide with A2. In **Fig. 12** (b), because of downward movement of girder (maximally 15.51 cm at 58.21s) and anti-clockwise movement of legs, girder might vibrate severely and suffer unseat from A2. Therefore, Span 4 would collapse entirely.

Therefore, failure mechanisms are summarized in **Fig. 13** and in **Fig. 14** for detail of A2. As shown in **Fig. 13** (a), due to severe damage at AL-4-R, IL-4-R and G-4-R and the opposite points on left, girder may move toward right and collide with A2 at first (corresponding to **Fig. 14** (a)). Due to this collision, backward movement and residual displacement may occur to A2. Then, with progress of local damage and further vibration, girder

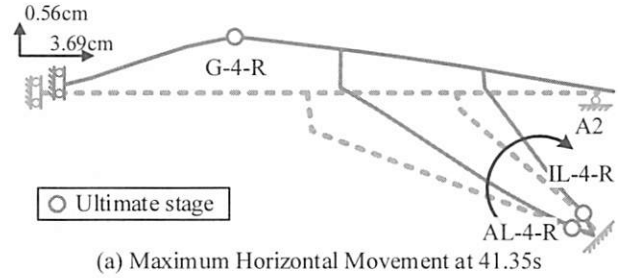

(a) Maximum Horizontal Movement at 41.35s

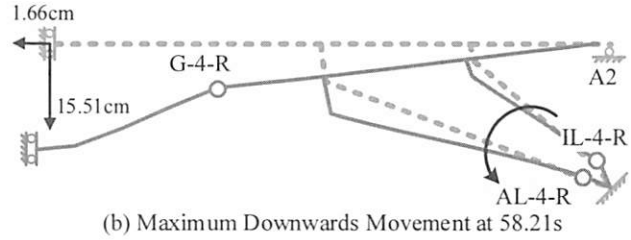

(b) Maximum Downwards Movement at 58.21s

Fig. 12 Failure to Span 4 According to Analytical Result

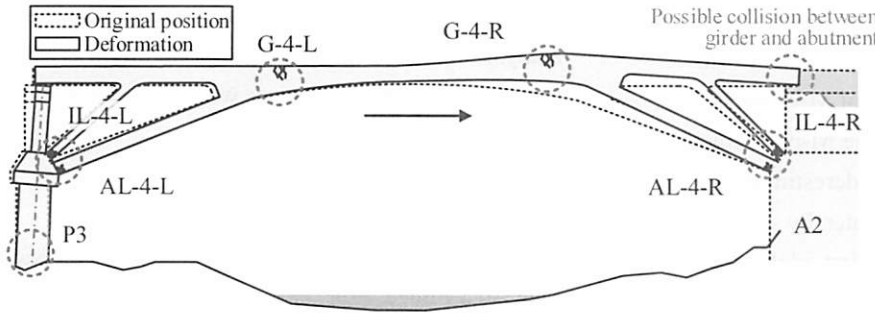

(a) Step 1: Horizontal Movement and Possible Collision

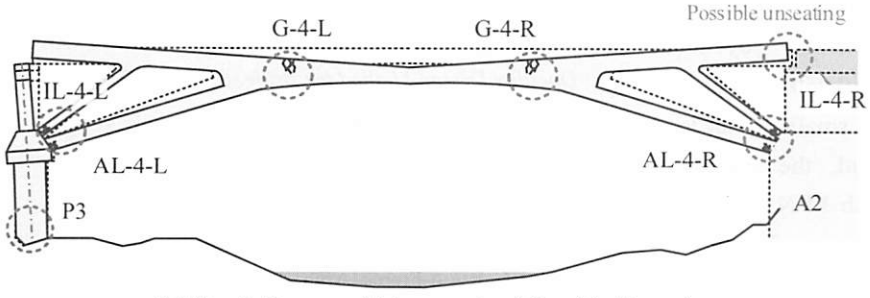

(b) Step 2: Downward Movement and Possible Unseating

Fig. 13 Possible Failure Mechanisms of Span 4

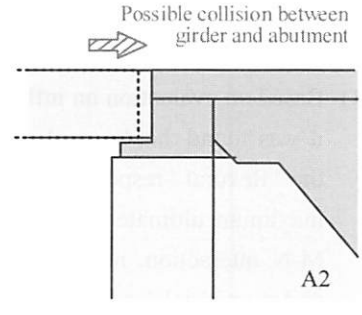

(a) Possible Collision

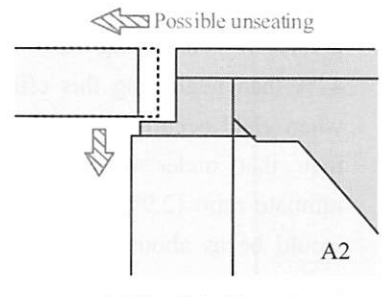

(b) Possible Unseating

Fig. 14 Detailed Mechanisms of A2

may move toward left and unseat from A2 consequently, as shown in **Fig. 13** (b) and **Fig. 14** (b). As a result, girder collapses entirely, and P3 tilts toward right. Span 3 would collapse after tilt of P3.

At last, actual damage and analytical result at bottom of right arch leg on Span 4 (AL-4-R) are compared in **Fig. 15** ((a) for position, (b) for section I-I, (c) for actual damage and (d) for analytical result). In actual damage, bottom of AL-4-R suffered severe damage (in **Fig. 15** (c)). Both core and surface concrete at 50cm from bottom (section I-I) crashed, while the longitudinal bars buckled but not broke off. According to analysis (ultimate ratio distribution from bottom shown in **Fig. 15** (d)), section I-I at bottom of AL-4-R would suffer extreme flexural damage of 2.991 times of Φ_u under high axial load. Besides, about 18cm (about 1/4 of sectional depth) from bottom exceeds the ultimate stage in analysis. Therefore, although the range that suffers damage of ultimate stage in analysis is smaller than actual damage after collapse of girder, the capacity loss of AL-4-R was able to be reappeared in the analysis. This suggests that the analysis considering the M-N interaction simulates the actual damage well, such as arch legs.

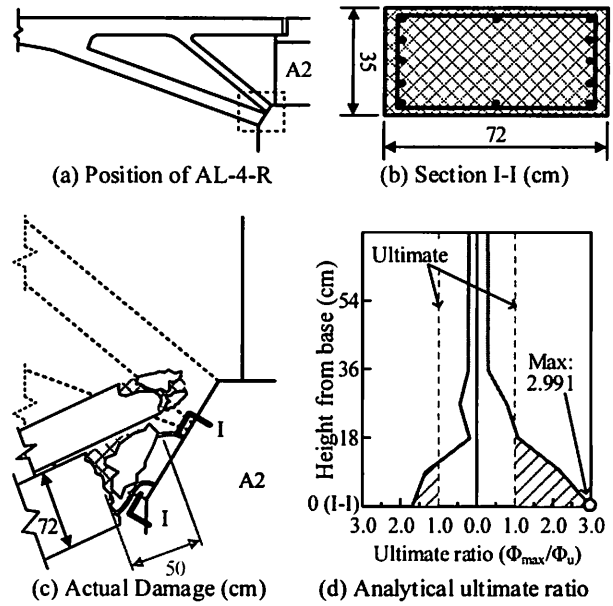

(a) Position of AL-4-R (b) Section I-I (cm)

(c) Actual Damage (cm) (d) Analytical ultimate ratio

Fig. 15 Actual Damage and Analytical Result (AL-4-R)

6. CONCLUSIONS

By dynamic analyses for Xiaoyudong Bridge for Span 3 & 4, focusing on influence by considering or neglecting M-N interaction, and the reasoning of possible failure mechanisms, following conclusions have been drawn:

(1) Based on evaluation on influence of M-N interaction, it was found that by neglecting the M-N interaction, the flexural response was underestimated. The maximum ultimate ratio was greater by considering M-N interaction, no matter the first yield occurred under an axial load greater or smaller, compared to the axial load by only dead load. The average maximum ultimate ratio of 4 points (1.710) was greater if considering M-N interaction , by about 44% than neglecting this effect (0.950). Especially when yield occurred early due to smaller axial load than that under only dead load, the maximum ultimate ratio (2.991) in case with M-N interaction would be as about 3.9 times great as that in case without M-N interaction (0.767).

(2) Subjected to extremely high axial load (maximally about 65% of axial capacity), arch legs on Span 3 & 4 suffered extensive failure, with peak ultimate ratio of 2.991. Being the main supporting member of this RC rigid-frame arch bridge, its sectional area was too small, and ductility was too low due to few ties.

(3) For failure mechanisms, due to ultimate stage at bottom of inclined leg, arch leg, and girder joints, the bridge would move notably. After possible collision with A2, girder of Span 4 might unseat from A2 by further vibration. As a consequence, the entire Span 4 would collapse and P3 would tilt towards right, followed by the failure of Span 3. In actual damage of AL-4-R, concrete at base 50cm crashed, and main bars buckled but not broke off. Although damage in analysis at bottom of arch leg was slightly less severe than actual, capacity loss was well reappeared.

REFERENCES

1) Ren, H. et al.: Inspection and Design Suggestion on Rigid-Frame Arch Bridge, *Proc. of the 1st Chinese-Croatian Joint Colloquium on Long Arch Bridge*, pp. 309-315, 2008

2) Inokuma. Y et al.: Seismic Design of A Steel-Concrete Composite Arch Bridge, *Proc. of the 1st Symposium on Ductility Design Method for Bridges*, pp. 241-244, 1998

3) Sakai, J. et al.: Seismic Response of A Reinforced Concrete Arch Bridge Taking Account of Axial Force and Moment Interaction, *Jr. of JSCE*, No. 724/I-62, pp. 69-81, 2003

4) Shi, Z. et al.: Seismic Damage Assessment-Based Analysis of a RC Rigid-Frame Arch Bridge Affected by Wenchuan Earthquake, *Jr. of Str. Eng., JSCE*, pp. 459-471, 2008